

# A novel Aloe Vera-Loaded Ethylcellulose/Hydroxypropyl Methylcellulose Nanofibrous Mat Designed For Wound Healing Application

Leila Yavari (✉ [yavarileyla7212@gmail.com](mailto:yavarileyla7212@gmail.com))

Tabriz University of Medical Sciences

Marjan Ghorbani

Tabriz University of Medical Sciences

---

## Research Article

**Keywords:** Electrospinning, Nanofibers, Wound healing, Hydroxypropyl methylcellulose, Ethyl cellulose, Aloe Vera

**Posted Date:** May 18th, 2021

**DOI:** <https://doi.org/10.21203/rs.3.rs-517639/v1>

**License:** © ⓘ This work is licensed under a Creative Commons Attribution 4.0 International License.

[Read Full License](#)

---

**Version of Record:** A version of this preprint was published at Journal of Polymers and the Environment on July 20th, 2021. See the published version at <https://doi.org/10.1007/s10924-021-02240-0>.

# Abstract

Newly, the usage of nanofibers (NFs) as wound dressings with the aim of their rapid healing and prevention of bacterial infection has been considered by researchers. In this regard, we produced the ethylcellulose/hydroxypropyl methylcellulose NFs incorporated with Aloe-vera (EC/HPMC/Alv) by the electrospinning technique. The produced NFs were investigated for their chemical structure, morphological, mechanical, thermal stability, degradation, swelling, cell viability, and antibacterial properties. Amongst the produced NFs, the NF samples containing 10% Alv illustrated the appropriate thermal stability and tensile properties. The produced NFs did not show any cell cytotoxicity which indicates their good compatibility. Also, NFs containing Alv significantly ( $P < 0.05$ ) increased cell proliferation and adhesion. In addition, the NFs/Alv sample was indicated antibacterial ability against *S. aureus* ( $10.21 \pm 1.21$  mm) and *E. coli* ( $5.06 \pm 1.3$  mm) pathogenic bacteria. As a result, these findings suggest that the produced NFs could be applied as an active mat for wound dressing application.

## 1. Introduction

The wound is known as skin damage caused by surgery or trauma, commonly [1]. Wound healing is a physiological complex and time-consuming process, which happens in four phases including; hemostasis, inflammation, proliferation, and regeneration [2, 3]. The main purpose of wound dressing is to heal, prevent bacterial infection, absorb wound exudate, and cellular regeneration [4]. Nowadays, the design of modern wound dressings has been studied and researched because weakness in wound dressings is a serious problem in wound healing [5]. The nanofibers produced through the electrospinning method have great attributes with the comparison to common wound dressing materials [6]. Polymeric nanofibers (NFs) have a high surface and a porous structure that are very important for absorbing wound exudates and can simulate the extracellular matrix [7]. In this regard, different polysaccharides and proteins have been applied to fabricate NFs mats for wound healing. Here, we produced a novel NFs based on the biocompatible cellulose derivative polymers. Cellulose can be applied as an appropriate choice for wound dressing formulas due to the easy extraction, biocompatibility, biodegradability, and safety [3]. Ethylcellulose (EC), is one of the cellulose derivatives, which it's an inert water-insoluble hydrophobic polymer suitable for sustained release systems [8, 9]. Hydroxypropyl methylcellulose (HPMC) is a water-soluble polymer used in the structure of NFs to absorb and retain liquids. Also, HPMC as an emulsifier and film-forming agent can be added to the hybrid polymer solution to improve and increase the stability of the electrospun NFs [10]. Moreover, antibacterial NFs can be produced with the encapsulation of antibacterial compounds to reduce the risk of infection [3, 7]. Aloe-Vera (Alv), is well known for its therapeutic potential, that widely used for the treatment of different dermatologic disorders, such as infections, burns, and other skin diseases [11]. The gel which resulted from Alv have abundant water that is very vital for wound hydration, also it has an antibacterial activity that can play an important role in the preventing infection [12, 13]. In conclusion, this study aimed to develop and characterize the Alv-loaded EC/HPMC electrospun NFs as a new antibacterial biomaterial for wound healing.

## 2. Materials And Methods

### 2.1. Materials

EC was purchased from Aladdin Chemistry Company. (Shanghai, China). Alv powder (decolorized) was purchased from Melbourne, Florida USA Company. HPMC, 3-(4,5-Dimethylthiazol-2-yl)-2,5-diphenyl tetrazolium bromide (MTT), fetal bovine serum (FBS), trypsin–EDTA, RPMI 1640 medium, Dimethyl sulfoxide (DMSO), and Phosphate buffered saline (PBS) were purchased from Sigma-Aldrich (St. Lo., USA), Ethanol 96%, and Muller Hinton Agar were purchased from Merck Chemical Co. (Darmstadt, Germany). The mouse embryonic fibroblast cell line (NIH-3T3), and Stock cultures, *Escherichia coli* (PTCC-1270), *Staphylococcus aureus* (PTCC-1112) were purchased from Pasture Institute (Iran).

### 2.2. Preparation of NFs

In short, HPMC and EC solution with concentration of 25 w/v% was prepared by the mixing of the EC (ethanol 80% v/v) and HPMC (acetic acid 70% v/v). EC/HPMC solution was prepared in three ratios of 95:5, 90:10, and 85:15 with stirring for 30 min. After that, Alv with ratios of 10% (versus total polymer weight) were encapsulated into optimal selected NFs. Then, the solutions (5 mL) were injected into the syringe (21gauge needle) by voltage ranged between 14 and 16 kV and flow rate of 1 mL/h. This procedure was completed at  $25 \pm 3^\circ\text{C}$  and  $30 \pm 2\%$  relative humidity [7].

### 2.3. Characterization of EC/HPMC/AV NFs

FT-IR spectra of NFs were recorded through a Thermo Avatar 370 spectrometer (Tensor27, Bruker Co., Ettlingen, Germany) to study the structural interactions of NFs. All spectra were recorded in the ranges of between 500 and  $4000\text{ cm}^{-1}$ . The Surface morphology of NFs after gold coating (DST1, Nanostructured Coating Co., Tehran, Iran) was studied with SEM (Philips XL 30 FEG, Amsterdam, Holland) at a voltage of 25 kV. The distribution of NFs diameters was specified with Image J analysis software. Moreover, the thermal stability of NFs was analyzed by TGA (TGA, Germany, Linseis, STA PT1600) at a range of 25-600 °C and heating rate of  $10\text{ }^\circ\text{C}/\text{min}$ .

### 2.4. Analysis of tensile property of NFs

The thickness of NFs was determined by a digital micrometer (Fowler, USA). After that, the tensile property of NFs in both dry and wet states was evaluated at room temperature using a Tensile Analyzer (Instron 5566, USA). The NFs were cut to dumbbell shape ( $3\text{ cm}\times 1\text{ cm}$ ) and then placed between two grips. The crosshead rate was established at  $0.04\text{ mm}/\text{s}$  [14].

### 2.5. Swelling degree

To determine the swelling degree of NF samples, gravimetric analysis was performed [15]. In summary, at first, the dry weight of the NFs was measured ( $W_d$ ), after that the NFs were immersed in 30 ml of PBS

solution at ambient temperature. Then, the swollen NFs were weighed after 5, 10, 15, 20, and 25 h ( $W_s$ ). The swelling degree (SD) was determined according to the Eq:

$$SD (\%) = \frac{W_s - W_d}{W_d} \times 100$$

## 2.6. Analysis of NFs degradation

The *in-vitro* degradation degree of NFs was measured using immersing NF samples in the PBS. The NFs were immersed in 30 mL of PBS solution (37 °C and pH 7.4, 5.3) for 24 days. The weight loss (WL) of the initially weighed NFs ( $W_0$ ) was calculated as a function of the immersing time in PBS. At specific times (3, 6, 12, 18, and 24 days), the samples were removed from the PBS and the excess water absorbed by lying the samples on the surfaces of a filter paper and weighed ( $W_t$ ). The WL degree was calculated using the Eq:

$$WL (\%) = \frac{W_0 - W_t}{W_0} \times 100$$

## 2.7. Cell proliferation and cell adhesion studies

The MTT technique was accomplished to explore the cell viability of NF samples [15, 16]. In short, the NF samples were cut into 12 mm<sup>2</sup> and sterilized by UV irradiation. After that, 1 mL of cell suspension including  $5 \times 10^4$  cells was dropped onto sterilized NF samples and incubated in RPMI-1640 including 10% FBS at 37 °C with 5% CO<sub>2</sub>. After 1, 3, and 5 days, 200 µL DMSO was added to dissolve formazan crystals formed inside cells. Then, the absorbance was determined using a spectrophotometer (UV-2550, Shimadzu, Japan) at 570 nm. To investigate the cell adhesion ability of produced NFs, the attached cells on the surface of samples were visualized using the SEM technique. In this regard, before the cell studies, optimal NF was sterilized with UV radiation around 10 min and then, the cells were placed on the surface of selected NFs sample and incubated as mentioned above. To image the cells attached to the surface of NFs, the cells were fixed using a glutaraldehyde solution (4%) and then, dehydrated with gradient drying with ethanol (30, 50, and 80%). As a result, the samples were stored at 4 °C to study with SEM analysis.

## 2.8. Antibacterial activity

To investigate the antibacterial behavior of NF samples, the agar disc diffusion assay was used against *S. aureus* and *E. coli* bacteria. Muller Hinton Agar (MHA) culture was prepared freshly and bacterial suspensions ( $1.5 \times 10^8$  CFU/mL) were cultured. After that, NF samples were cut with a diameter of 5 mm, exposed to MHA, and then incubated for 24 h at 37 °C. After that, the plates were surveyed for the inhibition zone of the NF disks. The inhibition regions formed by the NF samples were calculated by a caliper in two replications and reported as antibacterial activity [16].

## 2.9. Statistical analysis

Data were examined by GraphPad Prism 5. One-way variance (ANOVA) and Tukey's test were applied to examine the experimental value. Differences were considered significant at  $P < 0.05$ .

# 3. Results And Discussion

## 3.1. SEM analysis

The morphology of NF samples was studied with the SEM technique. The SEM results of NFs with different blending ratios of EC, HPMC and selected NF with encapsulated Alv were illustrated in Fig 1. The average diameter of NF samples was assessed using Image J software. By changing the blended ratio of EC/HPMC, the morphology of NFs was improved. As shown in Fig. 1, the average NFs diameter was reduced by changing the combination ratio of EC/HPMC from 95:5 to 90:10 and 85:15. The fiber diameters of EC/HPMC with the blended ratios of 95:5, 90:10, and 85:15 were in the ranges of  $601 \pm 234$ ,  $556 \pm 185$ , and  $527 \pm 136$  nm, respectively. This reduction of fiber diameter with increasing the amount of HPMC in NFs could be associated with the increased conductivity, causing larger elongation forces and reduction of fibers diameter, which is in accordance with the results of previous studies [10]. The NF sample with a blending ratio of 85:15 of EC/HPMC illustrated the uniform, thin, and without bead fibers. Therefore, the EC/HPMC 85:15 NF sample was selected as the optimal NFs for encapsulation of Alv, since it has an appropriate morphology and thin fibers. After the addition of Alv, the average fiber diameter significantly reduced ( $319 \pm 94.66$  nm). The SEM analysis of EC/HPMC/Alv indicated a regular and beadless morphology. This result was in accordance with the results of previous study [7]. These results indicated the high compatibility among the NFs matrix and Alv which provided an appropriate choice for encapsulation of Alv into this NFs matrix without adverse effect on the morphological characteristics.

## 3.2. FTIR analysis

The FTIR spectra of Alv, EC, HPMC, EC/HPMC, and EC/HPMC/Alv NFs were presented in Fig. 2. The FTIR spectrum of Alv indicated specific absorptions at  $1240 \text{ cm}^{-1}$  (stretching of C-O groups of esters and phenols),  $1560 \text{ cm}^{-1}$  (C=O stretching),  $1710 \text{ cm}^{-1}$  (presence of carbonyl groups),  $2910 \text{ cm}^{-1}$  (symmetrical and asymmetrical C-H stretching), and  $3311 \text{ cm}^{-1}$  related to the hydrogen-bonded N-H stretching [7]. The EC spectrum showed the peaks at  $1120 \text{ cm}^{-1}$  (-C-O-C- stretching), and  $2850\text{-}2962 \text{ cm}^{-1}$  (-CH<sub>3</sub> stretching) [9]. Furthermore, the peak at  $1745 \text{ cm}^{-1}$  was related to the stretching of C=O bonds [17]. FTIR spectrum of HPMC indicated the peaks at  $1641 \text{ cm}^{-1}$ ,  $1458 \text{ cm}^{-1}$  and  $1375 \text{ cm}^{-1}$  owing to the vibration of -OH group, asymmetric and symmetric vibrations of a methoxy group (-OCH<sub>3</sub>), respectively. Additionally, the peak at  $1052 \text{ cm}^{-1}$  was associated with the C-O-C stretching bond [18]. The FTIR spectrum of EC/HPMC exhibited the peaks at  $1746 \text{ cm}^{-1}$ ,  $1638 \text{ cm}^{-1}$ , and  $1123 \text{ cm}^{-1}$ , which indicates the suitable physical interactions between EC and HPMC. By comparing the FTIR spectrum of EC/HPMC, the

characteristic peaks of EC/HPMC/Alv NF samples had blue shifts ( $1746 \rightarrow 1753 \text{ cm}^{-1}$ ,  $1638 \rightarrow 1644 \text{ cm}^{-1}$ , and  $1123 \rightarrow 1183 \text{ cm}^{-1}$ ), showing the Alv was effectively encapsulated in the EC/HPMC NFs.

### 3.3. TGA analysis

Fig. 3, displayed the TGA thermograms of EC/HPMC NFs with various blending weight ratio of EC, HPMC, and optimal selected EC/HPMC NF samples containing 10% Alv. As can realize from this Fig, the first stage weight loss of NFs is between 50 and 150 °C which is related to the loss of free and bound water in the structure of NFs [19]. The second stage of weight loss occurred at the range of 150-380 °C which is associated to the thermal decomposition of the polymers [20]. Additionally, the next stage ranged between 380-600 °C can be related to the carbonization of polymeric materials [21]. There was not significantly difference in the thermal stability of NFs with different combination ratio of EC, and HPMC, indicating that the interactions between components were only physical rather than chemical interactions.

### 3.4. Mechanical properties

As shown in Table 1, the effect of different combination ratios of EC, HPMC (95:5, 90:10, and 85:15), and the encapsulation of Alv (10% w/v) into the EC/HPMC NFs was studied with the tensile stress (TS) analysis in the dry and wet conditions. The TS of NFs with various combination ratios of EC/HPMC in dry state was 4.96 MPa, 5.21 MPa, and 5.68 MPa for EC/HPMC 95:5, 90:10, and 85:15, respectively. These findings confirmed the TS improvement of EC-based NFs with the addition of HPMC. The encapsulation of Alv improved significantly ( $P < 0.05$ ) the TS up to 6.70 MPa that was owing to the interaction between NFs and Alv. Also, a comparable trend was observed for the TS of NFs in the wet state: 2.32 MPa, 3.11 MPa, and 3.40 MPa for the EC/HPMC with ratios of 95:5, 90:10, and 85:15, respectively. Additionally, the encapsulation of Alv led to enhance in the TS up to 4.23 MPa in the produced NFs. The refined TS of EC/HPMC by increasing the HPMC content and encapsulation of Alv into the NF structure can be due to the increased intermolecular interactions between polymer chains and Alv [22–24]. The obtained results showed that EC/HPMC/Alv NFs had sufficient TS to withstand the force applied to them and can be used as a wound dressing [25–27].

**Table 2.** Tensile stress (TS) analysis of Ethyl cellulose/Hydroxypropyl methylcellulose (EC/HPMC) with different blending ratios of 95:5, 90:10, and 85:15, and optimal EC/HPMC NFs (85:15) containing 10% Aloe Vera (Alv) in dry and wet state.

NF sample	TS (MPa) in dry state	TS (MPa) in wet state
EC/HPMC:95/5	4.96	2.32
EC/HPMC:90/10	5.21	3.11
EC/HPMC:85/15	5.68	3.40
EC/HPMC (85/15)/Alv (10 wt %)	6.70	4.23

### 3.5. Swelling degree

Swelling properties of produced NFs are very important to apply as a wound dressing [28]. The swelling degree of the EC/HPMC NF samples with various blending weight ratios (95:5, 90:10, and 85:15), and optimal EC/HPMC NF containing 10% Alv were calculated in PBS (pH 7.4) solution at 37 °C after 5, 10, 15, 20, and 25 h. Fig. 4, presented the swelling degree of NF samples. As can be seen from this Fig, the swelling ratio of NF samples increased over time particularly after 2 h with increasing the HPMC content and encapsulated Alv in NF samples. This result can be related to the formation of hydrogen bonds between the EC and HPMC, and also the ability to absorb and retain water by HPMC and Alv. Besides, increasing the HPMC content and encapsulation of Alv in NFs reduces the diameter of NFs and increases the porosity, which ultimately increases the ability to absorb and retain water [3, 15, 29, 30].

### 3.6. *In vitro* degradation studies

The degradation degree of EC/HPMC NFs with different blending ratios of 95:5, 90:10, and 85:15 were investigated as a function of incubation time at two different pH values (7.4, and 5.3). The produced NFs were degraded during 24 days. Depending on the combination ratios, the produced EC/HPMC NFs was illustrated the various degradation degree. As shown in Fig. 5, the order of the weight loss of EC/HPMC NFs with various blending ratio of EC, and HPMC was found as 85:15 > 90:10 > 95:5. These observations showed that with increasing HPMC content, the degradation degree also increases. This obtained result can be related to the reduction of the diameter of NFs with increasing HPMC content since it has been confirmed in previous studies that by the decreasing of the NF diameter and increasing the ratio of surface to volume, water penetration increases, thus the degradation degree also increases [3, 31, 32]. Furthermore, improving the degradation of NFs with increasing the content of HPMC may also be related to the hydrophilicity nature of HPMC. The produced NFs containing Alv indicated the highest degradation degree compared with other NFs, resulting in around 35% of its initial weight was dropped after 24 days. This result could be related to Alv's ability to improve the hydrophilicity nature and water uptake of NFs, which could be the reason for the increased degradation degree [33]. Therefore, we can adjust the NFs degradation with the changing of the EC/HPMC combination ratio by the electrospinning method to be suitable for usage as a wound dressing. Additionally, the degradation degree could be affected by the change of pH value. As is clear in Fig. 5, the degradation degree of NFs in acidic pH (5.3) was more than that physiological pH (7.4). It should be noted that the degradation process of HPMC is based on a hydrolytic reaction. In the presence of water, the etheric bonds in the structure of HPMC are broken. Thus the length of the degradation chains becomes shorter and the shorter parts dissolve in water [34]. Thus, EC / HPMC NFs with higher HPMC content were more degraded. The weight loss of NFs with various combination ratios of EC/HPMC at acidic pH (5.3) was around 37%, 34%, and 29% for EC/HPMC 95:5, 90:10, and 85:15, respectively.

### 3.7. Cell proliferation and cell adhesion studies

The NIH-3T3 cell viability was assessed in the presence of EC/HPMC NFs with and without Alv content by the MTT assay after 1, 3, and 5 days. The results of this test were displayed in Fig. 6. The obtained

results showed that there was no toxicity and these NFs enhanced cell proliferation. Also, the encapsulation of Alv into NFs due to the presence of glycoproteins in Alv structure has increased cell proliferation by up to 126%, which is in line with the reported previous literature [35–37]. The adhesion of NIH-3T3 cells on optimal EC/HPMC (85:15) NFs containing 10% Alv were shown with SEM technique after 1, 3, and 5 days. As shown in this Fig, the cell proliferation rate significantly depends on the hydrophilicity of the NFs [35].

The results of cell adhesion were presented in Fig. 7. As revealed in this Fig, NIH-3T3 cells were attached well on the surface of EC/HPMC/Alv NFs which illustrated good interaction between the NFs and the cells. Hydroxyl groups in HPMC polymer chains and Alv agent can increase the adhesion strength. These obtained results suggest that the encapsulation of Alv in the NFs provides an appropriate environment for cell viability and adhesion. This result could be related to the ability of Alv to improve the hydrophilicity nature and protein absorption of the NFs, which ultimately increase cell adhesion and proliferation [33, 38–40].

### 3.8. Antibacterial activity

To investigate the antibacterial ability of Alv (versus total polymer weight) loaded in NFs, the agar disc diffusion assay was used, which is founded on the amount of clear zone including a circular NF disk. The obtained results indicated that the control NFs did not inhibit the growth of the pathogenic bacteria. As shown in Fig. 8, *E. coli* (gram-negative bacteria), and *S. aureus* (gram- positive bacteria) were significantly ( $P < 0.05$ ) sensitive to Alv. In accordance, the diameter of the clear zone was  $10.21 \pm 1.21$  mm for *S. aureus* and  $5.06 \pm 1.3$  mm for *E. coli* bacteria. The obtained results were consistent with the results of previous studies that investigating the antimicrobial activity of Alv [13, 40–44].

## Conclusion

The Alv loaded EC/HPMC NFs were successfully produced by the electrospinning technique. The produced NFs were investigated for their chemical structure, morphological, mechanical, thermal stability, degradation, swelling, cell viability, and antibacterial properties. As obtained results, the NFs showed a homogeneous morphology that with increasing the content of HPMC, a decrease in the diameter of NFs was observed. This reduction in the diameter and increase in the porosity of NFs offer an effective role in increasing the swelling and degradation degree. The biocompatibility of produced NFs was confirmed using the *in-vitro* cell cytotoxicity evaluation. Besides, the EC/HPMC NFs containing 10% Alv indicated the more cell proliferation, adhesion, and antibacterial activity. As a result, these findings suggest that the produced NFs can be applied as active NFs for wound healing application.

## Declarations

## Acknowledgment



This research was supported by the Nutrition Research Center, Tabriz University of Medical Sciences (Grant number: 67160).

## References

1. El-aassar MR, Ibrahim OM, Fouda MMG et al (2020) Wound healing of nanofiber comprising Polygalacturonic / Hyaluronic acid embedded silver nanoparticles: In-vitro and in-vivo studies. *Carbohydr Polym* 238:116175. doi:10.1016/j.carbpol.2020.116175
2. Okur ME, Karantas ID, Şenyiğit Z et al (2020) Title page Recent trends on wound management; new therapeutic choices based on polymeric carriers Department of Pharmaceutical Technology, Faculty of Pharmacy, İzmir Katip Çelebi Abstract : Wound healing is an unmet therapeutic challenge among medical. *Asian J Pharm Sci* 0–84. doi:10.1016/j.ajps.2019.11.008
3. Ahmadian S, Ghorbani M, Mahmoodzadeh F (2020) International Journal of Biological Macromolecules Silver sulfadiazine-loaded electrospun ethyl cellulose / polylactic acid / collagen nano fi brous mats with antibacterial properties for wound healing. *Int J Biol Macromol* 162:1555–1565. doi:10.1016/j.ijbiomac.2020.08.059
4. Wahab A, Ogasawara H, Soo I, Ni Q (2019) Polyvinyl alcohol nanofiber based three phase wound dressings for sustained wound healing applications Polyvinyl alcohol nanofiber based three phase wound dressings for sustained wound healing applications. *Mater Lett* 241:168–171. doi:10.1016/j.matlet.2019.01.084
5. Liu M, Duan XP, Li YM et al (2017) Electrospun nanofibers for wound healing. *Mater Sci Eng C* 76:1413–1423. doi:10.1016/j.msec.2017.03.034
6. Akrami M, Tayebi L, Ghorbani M (2020) Curcumin-loaded naturally-based nanofibers as active wound dressing mats: Morphology, drug release, cell proliferation and cell adhesion studies. *New J Chem*. doi:10.1039/d0nj01594f
7. Ghorbani M, Nezhad-Mokhtari P, Ramazani S (2020) Aloe vera-loaded nanofibrous scaffold based on Zein/Polycaprolactone/Collagen for wound healing. *Int J Biol Macromol*
8. Yu DG, Wang X, Li XY et al (2013) *Acta Biomaterialia* Electrospun biphasic drug release polyvinylpyrrolidone / ethyl cellulose core / sheath nanofibers. 9:5665–5672. doi: 10.1016/j.actbio.2012.10.021
9. Wang P, Li Y, Zhang C et al (2020) Sequential electrospinning of multilayer ethylcellulose / gelatin / ethylcellulose nano fi brous fi lm for sustained release of curcumin. *Food Chem* 308:125599. doi:10.1016/j.foodchem.2019.125599
10. Bilbao-sainz C, Chiou B, Valenzuela-medina D et al (2014) Solution blow spun poly (lactic acid)/ hydroxypropyl methylcellulose nanofibers with antimicrobial properties. *Eur Polym J* 54:1–10. doi:10.1016/j.eurpolymj.2014.02.004
11. Maan AA, Nazir A, Khan MKI et al (2018) The therapeutic properties and applications of aloe vera: a review. *J Herb Med* 12:1–10

12. Naseri-nosar M, Farzamfar S (2017) Erythropoietin / aloe polyvinyl alcohol / chitosan sponge-like wound dressing: In vitro and in vivo studies. 1–13. doi: 10.1177/0883911517731793
13. Baghersad S, Bahrami SH, Mohammadi MR et al (2018) Development of biodegradable electrospun gelatin/aloe-vera/poly ( $\epsilon$ -caprolactone) hybrid nanofibrous scaffold for application as skin substitutes. *Mater Sci Eng C* 93:367–379
14. Paimushin VN, Firsov VA, Shishkin VM et al (2020) Erratum to: An Investigation into the ASTM E756-05 Test Standard Accuracy on Determining the Damping Properties of Materials in Tension-Compression. 63:420066
15. Ghorbani M, Mahmoodzadeh F, Yavari L, Nezhad-mokhtari P (2020) International Journal of Biological Macromolecules Electrospun tetracycline hydrochloride loaded zein / gum tragacanth / poly lactic acid nano fi bers for biomedical application. 165:1312–1322. doi: 10.1016/j.ijbiomac.2020.09.225
16. Yavari L, Ghorbani M (2021) International Journal of Biological Macromolecules Injectable chitosan-quince seed gum hydrogels encapsulated with curcumin loaded-halloysite nanotubes designed for tissue engineering application. 177:485–494. doi: 10.1016/j.ijbiomac.2021.02.113
17. Shi J, Liu W (2020) Preparation of cellulose nanocrystal from tobacco-stem and its application in ethyl cellulose film as a reinforcing agent. *Cellulose* 27:1393–1406. doi:10.1007/s10570-019-02904-0
18. Dharmalingam K, Anandalakshmi R (2019) International Journal of Biological Macromolecules Fabrication, characterization and drug loading ef fi ciency of citric acid crosslinked NaCMC-HPMC hydrogel fi lms for wound healing drug delivery applications. *Int J Biol Macromol* 134:815–829. doi:10.1016/j.ijbiomac.2019.05.027
19. Amjadi S, Emaminia S, Nazari M et al (2019) Application of Reinforced ZnO Nanoparticle-Incorporated Gelatin Bionanocomposite Film with Chitosan Nanofiber for Packaging of Chicken Fillet and Cheese as Food Models. *Food Bioprocess Technol* 12:1205–1219. doi:10.1007/s11947-019-02286-y
20. Ghorbani M, Roshangar L, Soleimani J (2020) Development of reinforced chitosan / pectin sca ff old by using the cellulose nanocrystals as nano fi llers: An injectable hydrogel for tissue engineering. *Eur Polym J* 130:109697. doi:10.1016/j.eurpolymj.2020.109697
21. Rostami M, Ghorbani M, Aman M et al (2019) International Journal of Biological Macromolecules Development of resveratrol loaded chitosan-gellan nano fi ber as a novel gastrointestinal delivery system. *Int J Biol Macromol* 135:698–705. doi:10.1016/j.ijbiomac.2019.05.187
22. Rad ZP, Mokhtari J, Abbasi M (2018) Fabrication and characterization of PCL/zein/gum arabic electrospun nanocomposite scaffold for skin tissue engineering. *Mater Sci Eng C* 93:356–366
23. Unnithan AR, Gnanasekaran G, Sathishkumar Y et al (2014) Electrospun antibacterial polyurethane-cellulose acetate-zein composite mats for wound dressing. *Carbohydr Polym* 102:884–892
24. Ghorbani M, Mahmoodzadeh F, Yavari Maroufi L, Nezhad-Mokhtari P (2020) Electrospun tetracycline hydrochloride loaded zein/gum tragacanth/poly lactic acid nanofibers for biomedical application. *Int*

- J Biol Macromol 165:1312–1322. doi:<https://doi.org/10.1016/j.ijbiomac.2020.09.225>
25. Peh K, Khan T, Ch'ng H (2000) Mechanical, bioadhesive strength and biological evaluations of chitosan films for wound dressing. *J Pharm Pharm Sci* 3:303–311
  26. Cui S, Sun X, Li K et al (2019) Polylactide nanofibers delivering doxycycline for chronic wound treatment. *Mater Sci Eng C* 104:. doi:10.1016/j.msec.2019.109745
  27. Zaman HU, Islam JMM, Khan MA, Khan RA (2011) Physico-mechanical properties of wound dressing material and its biomedical application. *J Mech Behav Biomed Mater* 4:1369–1375. doi:10.1016/j.jmbbm.2011.05.007
  28. El-aassar MR, El-beheri NG, Agwa MM et al (2021) International Journal of Biological Macromolecules Antibiotic-free combinational hyaluronic acid blend nano fi bers for wound healing enhancement. *Int J Biol Macromol* 167:1552–1563. doi:10.1016/j.ijbiomac.2020.11.109
  29. Bakhsheshi-rad HR, Fauzi A, Aziz M et al (2020) International Journal of Biological Macromolecules Development of the PVA / CS nano fi bers containing silk protein sericin as a wound dressing: In vitro and in vivo assessment. *Int J Biol Macromol* 149:513–521. doi:10.1016/j.ijbiomac.2020.01.139
  30. Aydogdu A, Sumnu G, Sahin S (2017) A novel electrospun hydroxypropyl methylcellulose / polyethylene oxide blend nanofibers: Morphology and physicochemical properties A novel electrospun hydroxypropyl methylcellulose / polyethylene oxide blend nano fi bers : Morphology and physicochemical. *Carbohydr Polym* 181:234–246. doi:10.1016/j.carbpol.2017.10.071
  31. Bölgen N, Menciloğlu YZ, Acatay K et al (2005) In vitro and in vivo degradation of non-woven materials made of poly ( $\epsilon$ -caprolactone) nanofibers prepared by electrospinning under different conditions. *J Biomater Sci Polym Ed* 16:1537–1555
  32. Agarwal S, Wendorff JH, Greiner A (2008) Use of electrospinning technique for biomedical applications. *Polymer* 49:5603–5621. doi:10.1016/j.polymer.2008.09.014
  33. Gainza G, Gutierrez FB, Aguirre JJ et al (2016) NOVEL NANOFIBROUS DRESSINGS CONTAINING rhEGF AND Aloe vera FOR WOUND HEALING APPLICATIONS. *Int J Pharm.* doi:10.1016/j.ijpharm.2016.11.006
  34. Li S, McCarthy S (1999) Further investigations on the hydrolytic degradation of poly (DL-lactide). *Biomaterials* 20:35–44
  35. Ju YM, Park K, Son JS et al (2007) Beneficial Effect of Hydrophilized Porous Polymer Scaffolds in Tissue-Engineered Cartilage Formation. doi: 10.1002/jbm.b.30943
  36. Jithendra P, Rajam AM, Kalaivani T et al (2013) Preparation and characterization of aloe vera blended collagen-chitosan composite scaffold for tissue engineering applications. *ACS Appl Mater Interfaces* 5:7291–7298
  37. Naseri-Nosar M, Farzamfar S, Salehi M et al (2018) Erythropoietin/aloe vera-releasing wet-electrospun polyvinyl alcohol/chitosan sponge-like wound dressing: In vitro and in vivo studies. *J Bioact Compat Polym* 33:269–281
  38. Ezhilarasu H, Ramalingam R, Dhand C (2019) Biocompatible Aloe vera and Tetracycline Hydrochloride. Loaded Hybrid Nanofibrous Sca ff olds for Skin Tissue Engineering

39. Frankova J, Salem AA, Sahffie NM et al (2020) Chitosan-Glucan Complex Hollow Fibers Reinforced Collagen Wound Dressing Embedded with Aloe vera. II. Multifunctional Properties to Promote Cutaneous Wound Healing. *Int J Pharm* 119349. doi:10.1016/j.ijpharm.2020.119349
40. Radha MH, Laxmipriya NP (2015) *Journal of Traditional and Complementary Medicine* Evaluation of biological properties and clinical effectiveness of Aloe vera: A systematic review. 5:21–26. doi: 10.1016/j.jtcme.2014.10.006
41. Miguel SP, Ribeiro MP, Coutinho P, Correia IJ (2017) Electrospun polycaprolactone/aloe vera\_chitosan nanofibrous asymmetric membranes aimed for wound healing applications. *Polymers (Basel)* 9:183
42. Danish P, Ali Q, Mm H, Malik A (2020) ANTIFUNGAL AND ANTIBACTERIAL ACTIVITY OF ALOE VERAPLANT EXTRACT
43. Aghamohamadi N, Sharifi N, Faridi R, Ahmad S (2019) Preparation and characterization of Aloe vera acetate and electrospinning fibers as promising antibacterial properties materials. *Mater Sci Eng C* 94:445–452. doi:10.1016/j.msec.2018.09.058
44. Nadiger VG, Shukla SR (2016) Antibacterial properties of silk fabric treated with Aloe Vera and silver nanoparticles. 5000:. doi: 10.1080/00405000.2016.1167391

## Figures

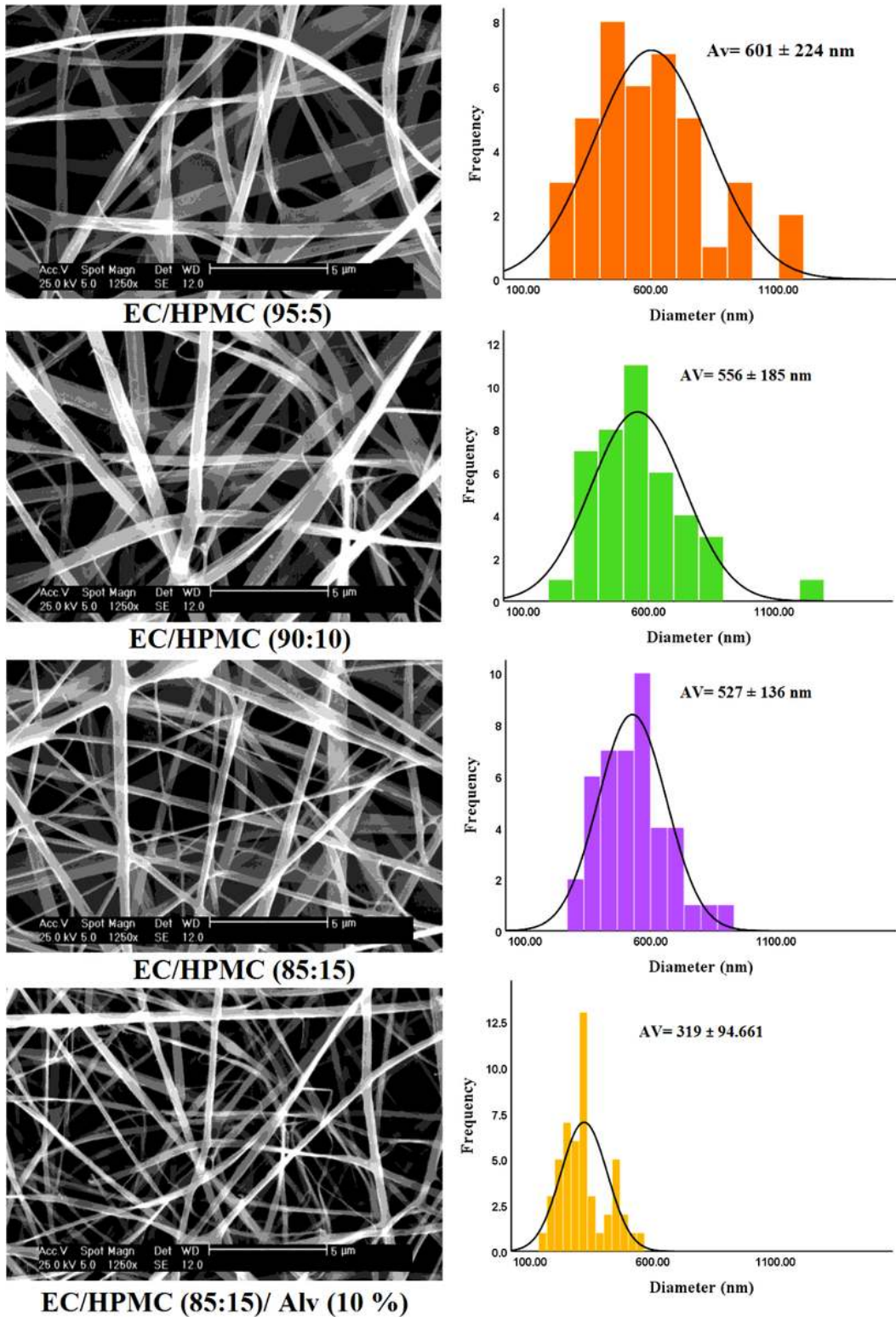


**Figure 1**

Fiber diameter distributions with average fiber diameter of Ethyl cellulose/Hydroxypropyl methylcellulose (EC/HPMC) with different blending ratios of 95:5, 90:10, and 85:15, and optimal EC/HPMC NFs (85:15) with 10% Aloe Vera (Alv). Data are expressed as mean  $\pm$  SD ( $n = 100$ ). Differences were considered significant at  $P < 0.05$ .

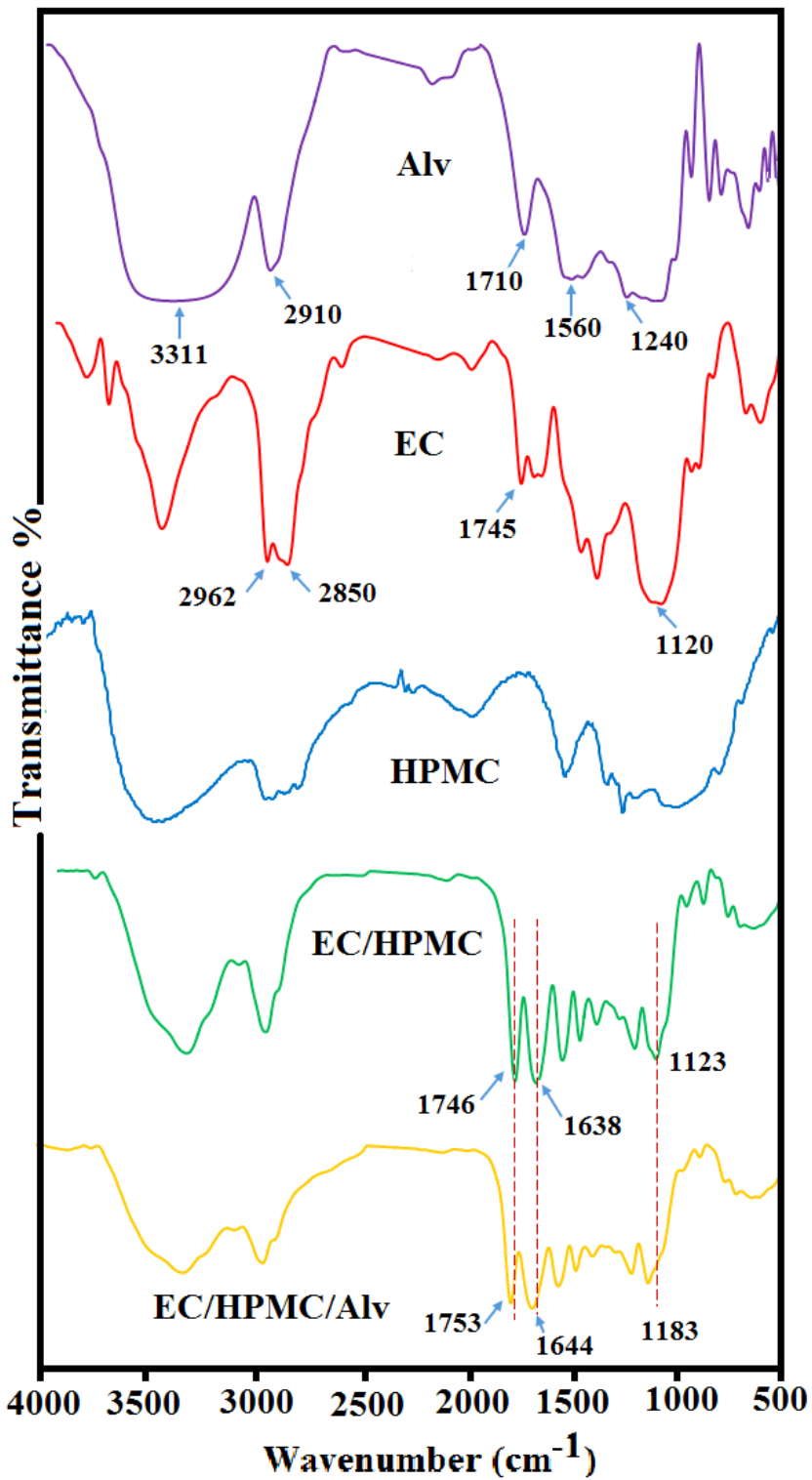


Figure 2

Fourier transform infrared (FTIR) spectra of Aleo-vera (Alv), Ethyl cellulose (EC), Hydroxypropyl methylcellulose (HPMC), EC/HPMC, and EC/HPMC/Alv nanofibers.

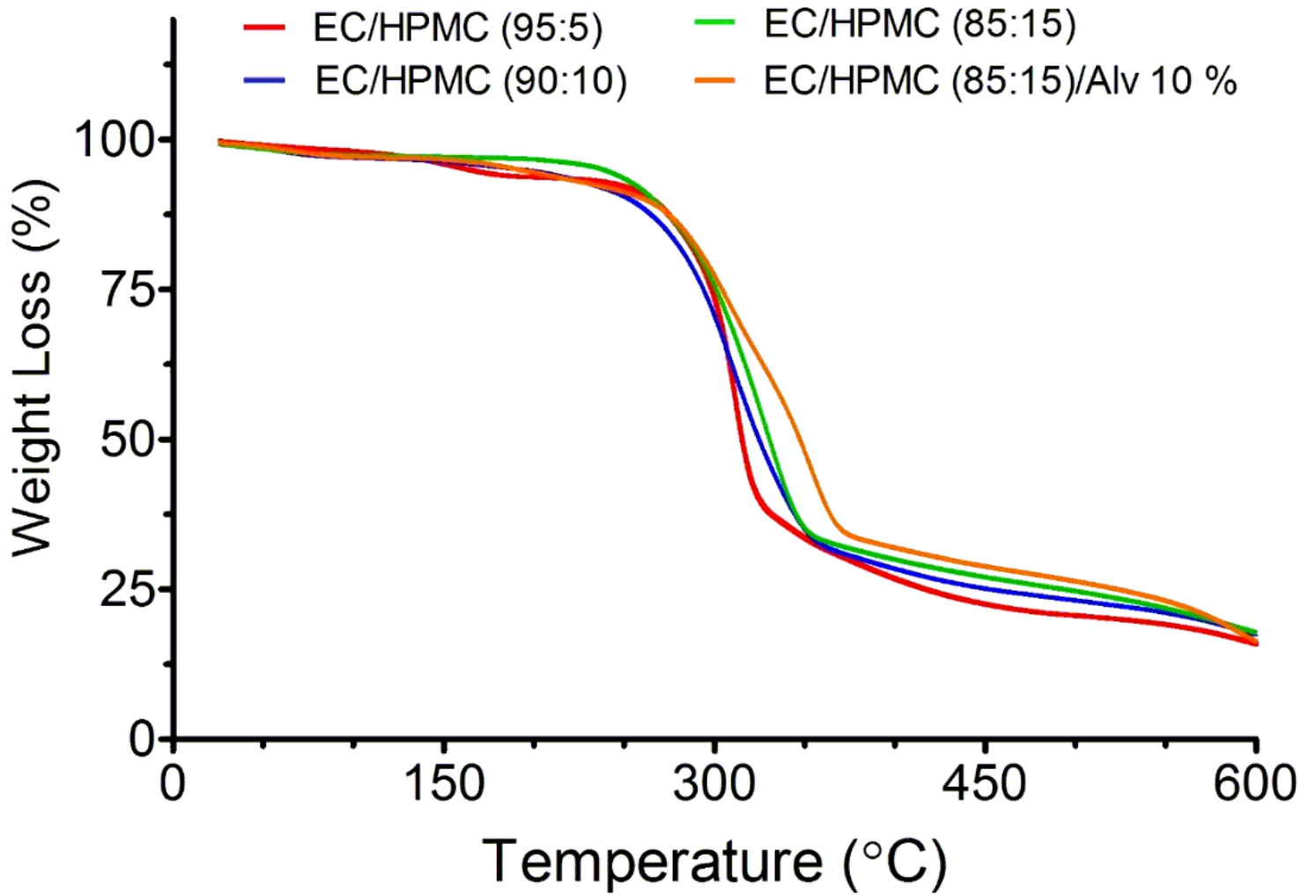


Figure 3

Thermogravimetric analysis (TGA) of Ethyl cellulose/Hydroxypropyl methylcellulose (EC/HPMC) with different blending ratios of 95:5, 90:10, and 85:15, and optimal EC/HPMC NFs (85:15) containing 10% Aloe Vera (Alv).

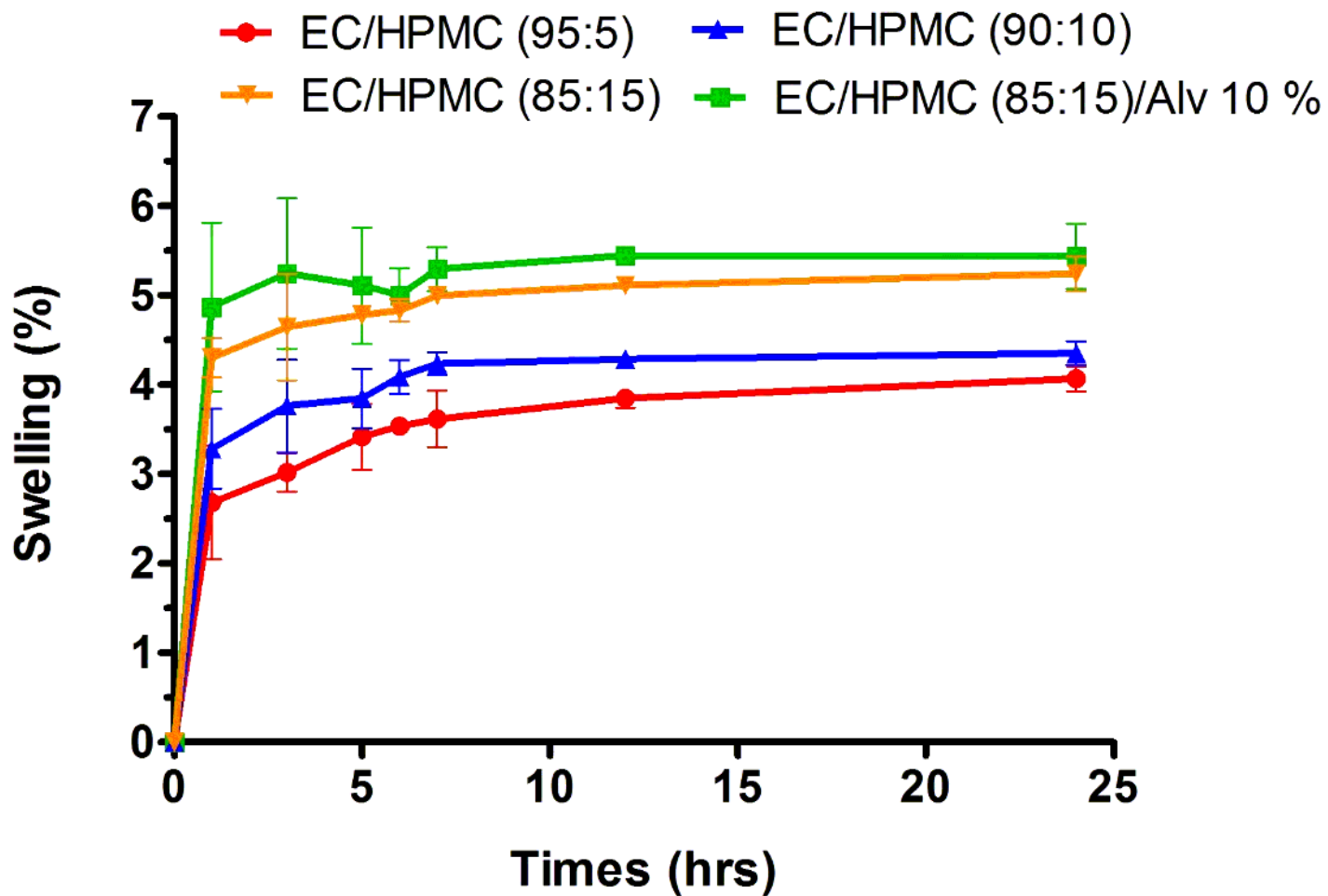


Figure 4

Swelling degree of Ethyl cellulose/Hydroxypropyl methylcellulose (EC/HPMC) with different blending ratios of 95:5, 90:10, and 85:15, and optimal EC/HPMC NFs (85:15) containing 10% Aloe Vera (Alv).

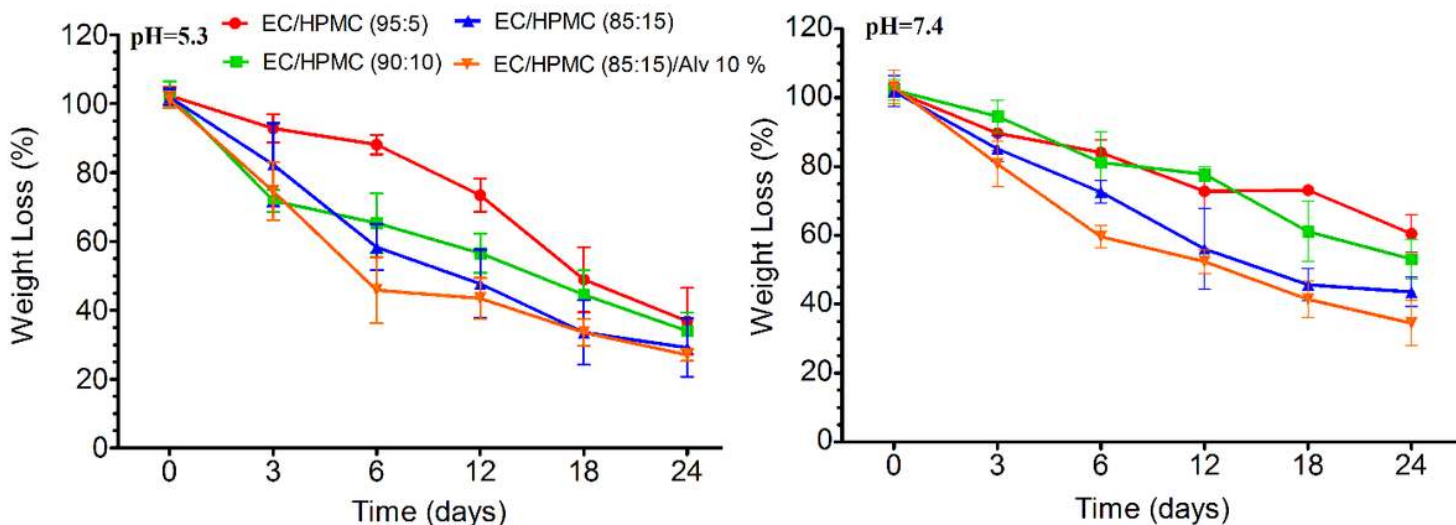


Figure 5



The degradation of Ethyl cellulose/Hydroxypropyl methylcellulose (EC/HPMC) with different blending ratios of 95:5, 90:10, and 85:15, and optimal EC/HPMC NFs (85:15) containing 10% Aloe Vera (Alv) in the pHs = 7.4, 5.3.

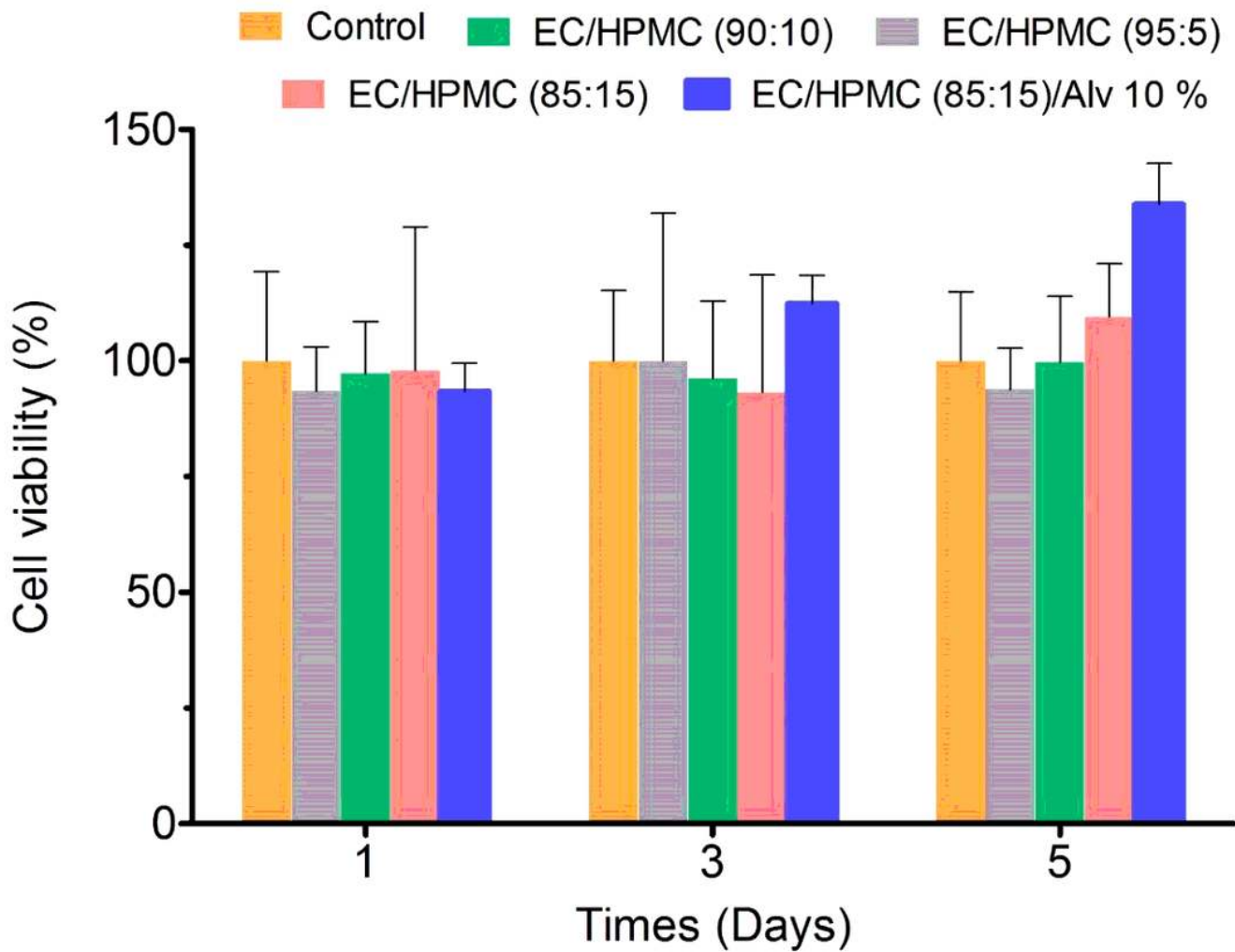


Figure 6

Cell viability of Ethyl cellulose/Hydroxypropyl methylcellulose (EC/HPMC) with different blending ratios of 95:5, 90:10, and 85:15, and optimal EC/HPMC NFs (85:15) containing 10% Aloe Vera (Alv).

**After 1 day**

**After 3 day**

**After 5 day**

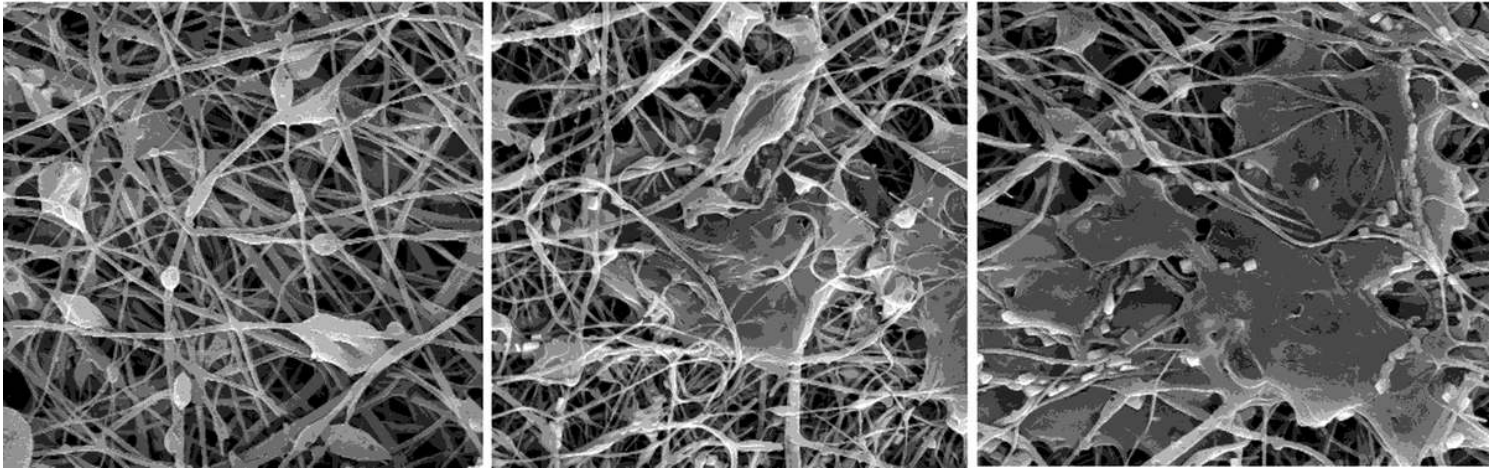


**Figure 7**

The cell adhesion of Ethyl cellulose/Hydroxypropyl methylcellulose (EC/HPMC) with blended ratio of 85:15 containing 10% Aloe Vera (Alv) after 1, 3, and 5 days.

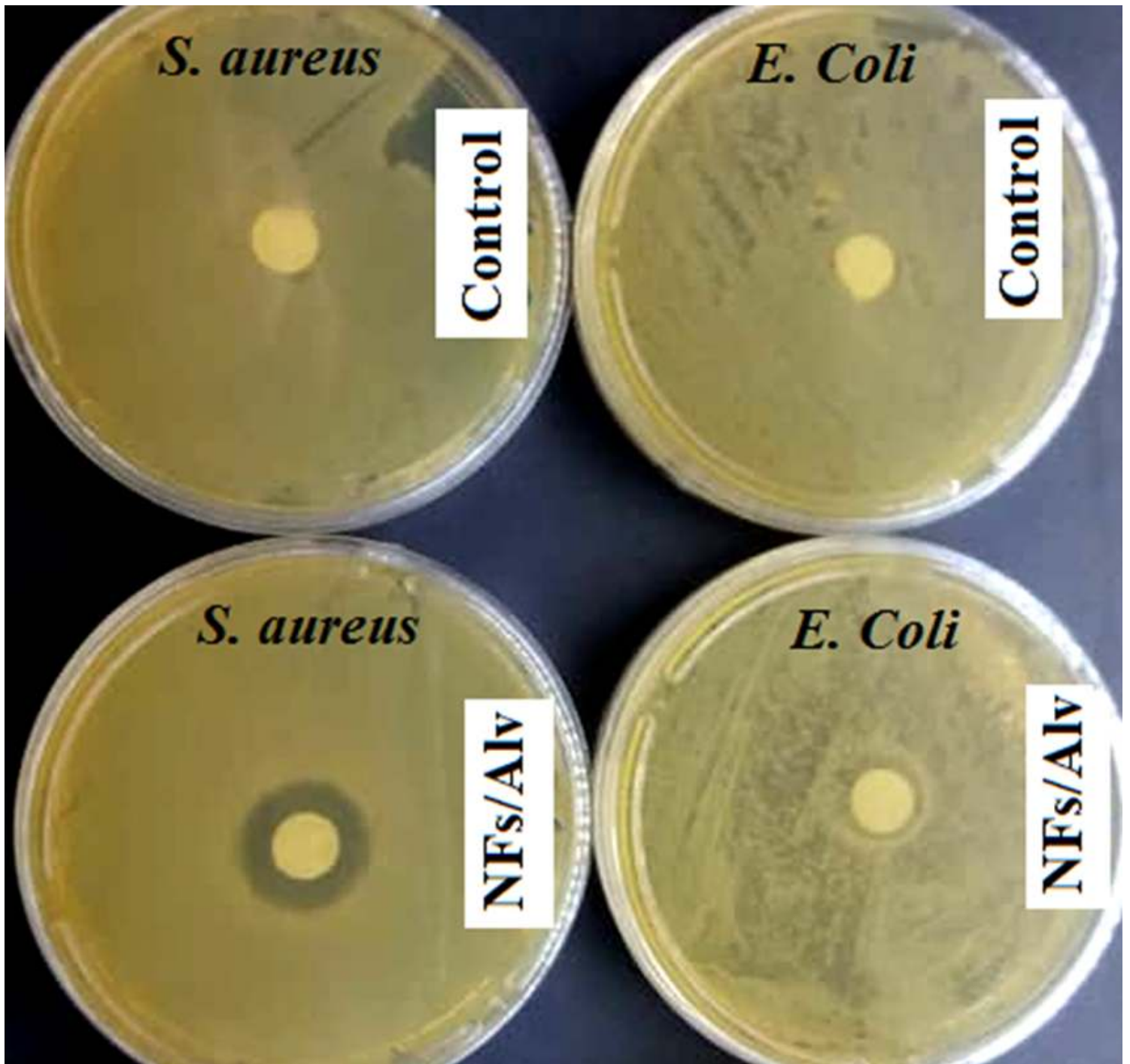


Figure 8

Antibacterial activity of Ethyl cellulose/Hydroxypropyl methylcellulose (EC/HPMC) with blended ratio of 85:15 (control), and control nanofiber (NF) sample containing 10% Aloe Vera (Alv) NFs.